

# Calculations of codoping effects between combinations of donors (P/As/Sb) and acceptors (B/Ga/In) in Si

Chihak Ahn<sup>a)</sup>

Department of Physics, University of Washington, Seattle, Washington 98195, USA

Scott T. Dunham

Department of Electrical Engineering, University of Washington, Seattle, Washington 98195, USA

(Received 10 September 2007; accepted 30 October 2007; published online 28 December 2007)

We studied codoping effects in silicon using first-principles calculations, with particular attention to charge compensation, Coulomb interactions, and strain compensation. We find that for B-doped systems, As or Sb counter doping reduces the maximum hole concentration, but that due to strong binding of multiple P atoms, Ga or In counter doping can increase electron density in heavily P-doped material. For acceptor-acceptor pairing, we find the B-B interaction to be repulsive as expected due to Coulombic effects, but calculations show a surprisingly significant attractive binding between B and In, which we attribute to hole localization. However, B-In binding is not promising for enhancing hole concentration since BIn pairs are deep acceptors. © 2007 American Institute of Physics. [DOI: 10.1063/1.2824942]

## I. INTRODUCTION

At the cutting edge of silicon technology, understanding interactions between multiple dopants is required to continue metal oxide semiconductor field-effect transistor (MOSFET) scaling. In modern ultralarge-scale integration (ULSI) technology, heavily codoped regions frequently occur, and it is observed that counter doping can be beneficial to reduce the junction depth.<sup>1-3</sup> There are two primary factors we consider for codoping effects: global strain compensation and local binding energy. Strain compensation between a small atom and a large atom can enhance the dopant segregation and reduce diffusivity,<sup>4-6</sup> and local binding also produces similar effects.<sup>3,7-9</sup> In codoping, a major component of local binding is the Coulomb interaction.

Experimentally, codoping can increase chemical concentration of dopants and retard dopant diffusion.<sup>3,7,10</sup> However, it is hard to separate out the effects of strain, electrostatics, and local chemical bonding from other dopant/defect interactions via experiment, since in many experimental setups there is no simple way to control individual effects. In our *ab initio* study, we separate strain energy and binding energy within the linear elasticity limit and investigate strain compensation and local binding individually.

## II. METHODS

We calculated the total free energy of 64-atom supercells, using the density functional theory (DFT) code Vienna *ab-initio* simulation package (VASP) (Ref. 11) in the generalized gradient approximation (GGA) with ultrasoft Vanderbilt-type pseudopotentials.<sup>12</sup> All B-related calculations were done with a 340 eV cutoff and all other calculations were done with a 250 eV cutoff. Throughout, 2<sup>3</sup> Monkhorst-Pack **k**-point sampling<sup>13</sup> was used. The convergence was tested for the same energy cutoff and **k**-points by

Diebel.<sup>14</sup> We minimized the finite-size effect via factoring out stress energy from the formation energy, and the validity of our calculations were tested using a 216-atom supercell for selected structures.

When donors and acceptors coexist in a silicon matrix, charge transfer occurs and band gap crossing should be taken into account in calculating the formation energy of donor-acceptor pairs in reference to neutral donors and acceptors. However, it is known that DFT is inaccurate in calculating band gaps.<sup>15</sup> To avoid this band gap crossing, we used charged donors and acceptors as reference states. For acceptor-acceptor pairs (e.g., BIn), neutral supercells were used as a reference, since there is no band gap crossing. The formation energy of a donor-acceptor pair can be given as

$$E_{MN}^f = E_{\text{Si}_{62}MN} - E_{\text{Si}_{63}M^+} - E_{\text{Si}_{63}N^-} + E_{\text{Si}_{64}}. \quad (1)$$

Table II lists the calculated formation energies. Since DFT underestimates the free energy of charged supercells,<sup>16</sup> the first-order Madelung correction was applied: ( $q^2\alpha/2\epsilon L \sim 0.16$  eV). For comparison, the two primary components of the formation energy, electrostatic energy and stress energy, are also listed in Table II.  $E^C$  is calculated by the monopole approximation, assuming a fully ionized donor and acceptor.

Within the elastic limit of a material, the free energy of a supercell can be represented as

$$E = E_0 + \frac{V}{2}(\boldsymbol{\epsilon} - x\Delta\boldsymbol{\epsilon})\mathbf{C}(\boldsymbol{\epsilon} - x\Delta\boldsymbol{\epsilon}), \quad (2)$$

where  $E_0$  is the minimum energy at relaxed lattice constant,  $V$  is the volume of the supercell,  $x$  is the atomic concentration of dopant,  $\boldsymbol{\epsilon}$  is applied strain,  $\Delta\boldsymbol{\epsilon}$  is the normalized induced strain (see Table I), and  $\mathbf{C}$  is the elastic stiffness tensor. The second term in Eq. (2) is the stress energy under normal stress. The binding energy is calculated by factoring out the stress energy from the formation energy using Eqs. (1) and (2), as listed in Table II.

<sup>a)</sup>Electronic mail: chahn@u.washington.edu.

TABLE I. Induced strain due to group III/V elements. The values are normalized to Si atomic volume and reported in reference to the GGA Si equilibrium lattice parameter of 5.457 Å.

	B	As	Sb	P	Ga	In
$\Delta\epsilon$	-0.30	0.018	0.18	-0.78	0.066	0.21

The binding energy of a donor-acceptor pair can increase solubility and retard diffusion as reported previously.<sup>3,7,17,18</sup>

For the dopants considered, we find the impact of the global strain compensation on solubility to be much smaller than the binding effects, even at a high counter-dopant concentration. To estimate the impact of ion pairing on charge carrier density, we calculated the pairing coefficient, the ratio between the total number of paired primary dopant atoms (e.g., B or P) and the total number of counter-dopant atoms,

$$P = \frac{N_{\text{primary}}^{\text{paired}}}{N_{\text{counter}}^{\text{total}}} = \frac{\sum_{i,m} i C_{im}}{\sum_{i,m} C_{im}}, \quad (3)$$

where  $C_{im}$  is the counter-dopant concentration containing  $i$  primary atoms and one counter atom. The index  $m$  is used to account for multiple combinations among the first-nearest neighbor (1NN), 2NN, and 3NN binding for the same  $i$ . Using the mass action law at equilibrium,  $C_{im}$  is given by

$$C_{im} = \Theta_{im} C_0 \left( \frac{C^{\text{free}}}{C_s} \right)^i \exp(-E_{im}^b/kT), \quad (4)$$

where  $\Theta_{im}$  is the configurational entropy factor,  $C_0$  is concentrations of unpaired counter dopant,  $C^{\text{free}}$  is the free primary dopant concentration,  $C_s$  is the silicon lattice concentration, and  $E_{im}^b$  is the binding energy of the given configuration.

Equations (3) and (4) are generally applicable to binding beyond 1NN, but much stronger binding at 1NN overwhelms the effect from a larger number of neighbors at 2NN and 3NN, even at high temperature. In addition, screening effects reduce the indirect binding energy beyond 1NN and at high doping concentrations, the screening length approaches the

TABLE II. Net formation energy of various ion pairs (eV). Except for 1NN, the sums of approximate Coulomb energy ( $E^C$ ) and strain compensation energy ( $E^S$ ) are within 0.15 eV of  $E^f$ . BAs 1NN pair shows weaker binding than Coulomb interaction, while InP pair shows much stronger binding.

		$E^f$	$E^S$	$E^C$
Si <sub>62</sub> BAs	1NN	-0.34	-0.02	-0.55
	2NN	-0.36	-0.02	-0.32
	3NN	-0.32	-0.02	-0.27
Si <sub>62</sub> BSb	1NN	-0.46	-0.08	-0.52
	2NN	-0.32	-0.08	-0.32
	3NN	-0.22	-0.08	-0.27
Si <sub>62</sub> GaP	1NN	-0.66	-0.008	-0.50
	2NN	-0.29	-0.003	-0.32
	3NN	-0.21	0.0	-0.27
Si <sub>62</sub> InP	1NN	-0.88	-0.02	-0.48
	2NN	-0.38	-0.02	-0.31
	3NN	-0.28	-0.02	-0.27

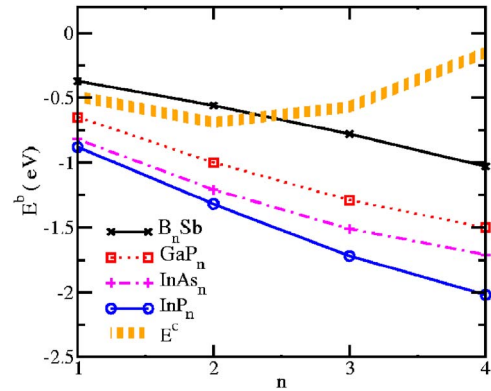


FIG. 1. (Color online) Energy for binding of multiple primary dopants to codopant. Thick orange line represents monopole Coulomb approximation.

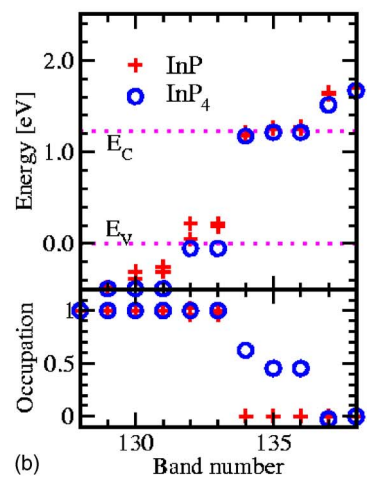
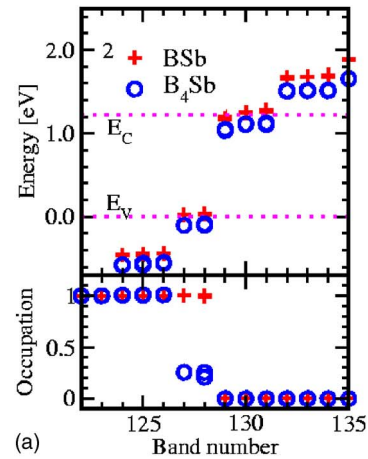


FIG. 2. (Color online) Density of states of donor-acceptor pairs with multiple binding. In contrast to B-Sb pairs, the energy levels associated with P near the top of the valence band are lowered significantly with P addition, which may account for the large binding energy of InP<sub>n</sub>. Dotted lines represent the conduction band minimum and valence band maximum for 2<sup>3</sup> k-point sampling.

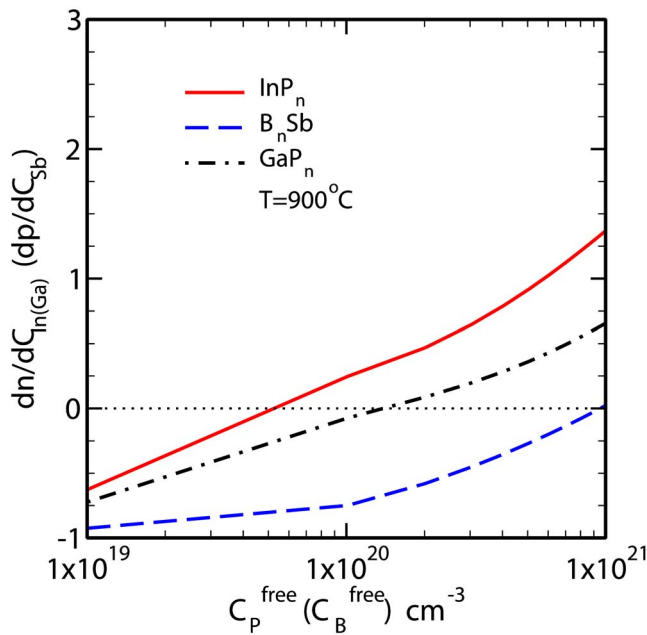


FIG. 3. (Color online) Differential free charge concentration per codopant atom as a function of concentration of free primary dopants. The number of paired B atoms per Sb atom is less than 1, which means BSb binding energy is not enough to overcome charge compensation. However, strong multiple binding between In and P may lead to enhanced electron charge density.

interatomic distance.<sup>19</sup> Thus,  $C_{im}$  can be simplified to  $C_i$  (the concentration of pairs with  $i$  primary dopant atoms at 1NN),

$$C_i = \frac{4!}{(4-i)! (i)!} C_0 \left( \frac{C_{\text{free}}}{C_s} \right)^i \exp(-E_i^b/kT). \quad (5)$$

The total majority carrier density is given by

$$n(\text{or } p) = C_{\text{primary}}^{\text{free}} + (P-1)C_{\text{counter}}^{\text{total}}, \quad (6)$$

where  $C_{\text{primary}}^{\text{free}}$  and  $C_{\text{counter}}^{\text{total}}$  are free primary dopant concentration and total counter-dopant concentration, respectively.

### III. RESULTS AND DISCUSSION

#### A. Donor-acceptor pairs

As listed in Table II, all the donor-acceptor pairs except pairs at 1NN show binding which is closely approximated by the sum of stress energy and Coulombic interactions. At least a portion of the modest difference between  $E^f$  and the sum of  $E^C$  and  $E^S$  (less than 0.15 eV) may arise from the inaccuracy of the point-charge approximation for the charged ions. We attribute the large energy discrepancy for donor-acceptor pairs at 1NN to direct local binding and higher order multipole interactions.

TABLE III. Formation energy of acceptor-acceptor pairs (eV). B-B interaction is repulsive, while BIn shows strong attractive binding.

	B <sub>2</sub>		BGa			BIn		
	1NN	1NN	2NN	3NN	1NN	2NN	3NN	
$E^f$	0.93	-0.06	-0.10	-0.08	-0.41	-0.29	-0.20	
$E^S$	0.28		-0.03			-0.10		
$E^b$	0.65	-0.03	-0.07	0.05	-0.31	-0.19	-0.10	

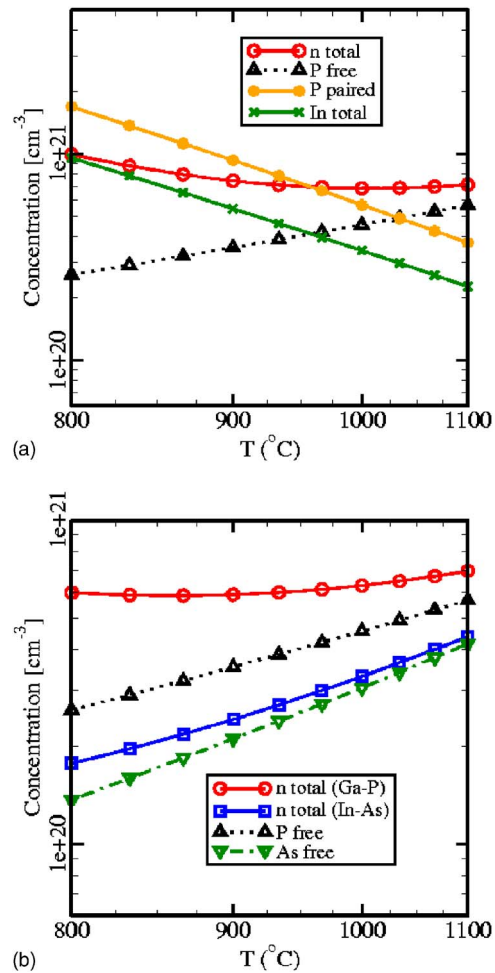


FIG. 4. (Color online) Total charge density as a function of temperature, with free dopant concentration taken as electrical solubility. Despite large As chemical solubility, pairing effect is modest due to smaller As electrical solubility compared to P. Electrical solubility of P and As was taken from Solmi *et al.* (Ref. 21) and Derdour *et al.* (Ref. 22), respectively. Ga and In solubility were taken from Refs. 23 and 24, respectively.

Figure 1 shows a monotonic increase in the binding strength as more dopants are bound to a counter dopant, which implies that the monopole Coulomb approximation clearly fails. It is notable that the binding energy of  $\text{InP}_n$  is quite large, while that of  $\text{B}_n\text{Sb}$  is much smaller. We believe that the strong binding between In and P is related to the In energy level lowering of initially deep In acceptor level when P binds to In (Fig. 2). Atoro *et al.* have suggested making In a shallow acceptor via a trimer with P ( $\text{In-P-In}$ ).<sup>20</sup>

Based on multiple binding between donors and acceptors, the differential carrier density (Fig. 3) and total carrier density (Fig. 4) due to counter doping were calculated. Fig-

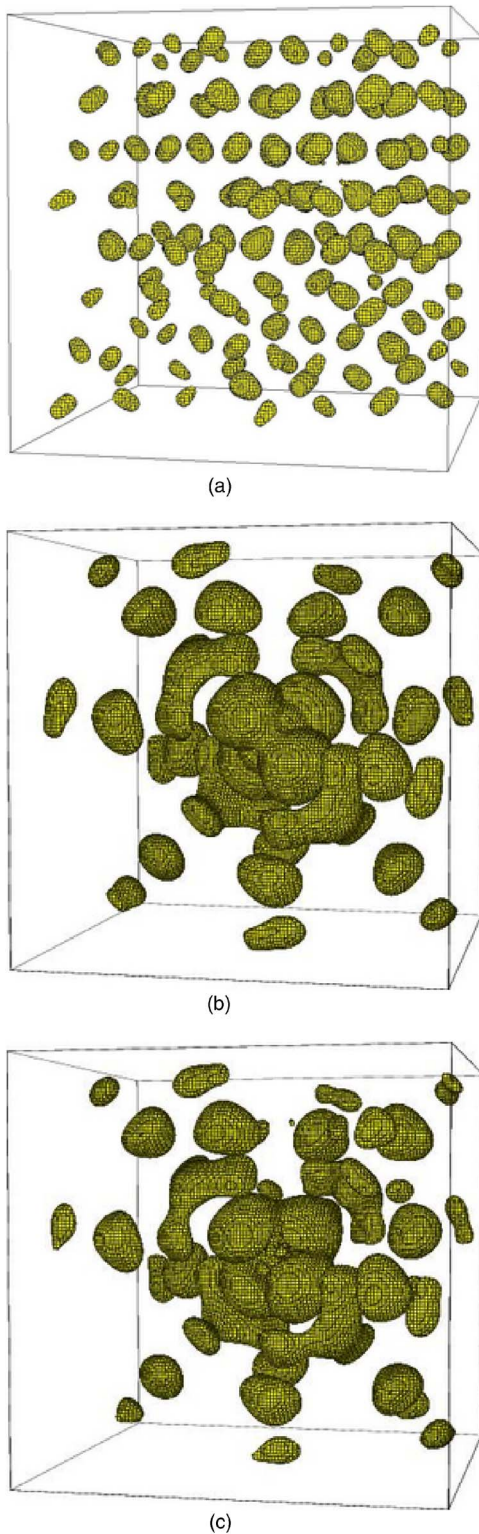


FIG. 5. (Color online) Hole density of (a) B, (b) In, and (c) BIn pair calculated by taking the difference of charge density between singly charged cell and neutral cell, showing hole localization for In and BIn. All isosurfaces were plotted at the same value of density ( $\Delta\rho=2.15 \times 10^{21} \text{ e/cm}^{-3}$ ).

ure 3 shows a change in carrier density as a function of free primary dopant (P or B). The negative value for  $B_n\text{Sb}$  up to well above the equilibrium B solubility implies that the binding is not strong enough to overcome the charge compensation between the donor and acceptor for this combination. Consistent with this prediction, Solmi *et al.* reported a reduc-

TABLE IV. Formation energy of BIn for various charge states (eV). When holes are removed, BIn interaction goes from attractive to repulsive.

	BIn	BIn <sup>-</sup>	BIn <sup>2-</sup>
$E^f$	-0.41	-0.21	0.12

tion in carrier densities due to B-Sb pairing.<sup>3</sup> For the case of  $\text{InP}_n$ ,  $dn/dC_{\text{In}}$  becomes positive well below P solubility. Though the In solubility is low ( $1.8 \times 10^{18} \text{ cm}^{-3}$ ) (Ref. 24) in pure silicon, pairing with P substantially increases the In solubility well above the normal value [Fig. 4(a)]. Ga-P pairing is also predicted to give a substantial activation enhancement, but due to the smaller As electrical solubility compared to P, the In-As pairing does not increase the total electron density significantly. Figure 4 was plotted assuming solubility of the counter dopant as free counter-dopant concentration. Counter doping and associated pairing can also be beneficial in formation of abrupt junctions by suppressing dopant diffusion.<sup>3,7,10</sup>

## B. Acceptor-acceptor pairs

When two acceptors are closely spaced, Coulomb repulsion is expected. Although this is true for two B atoms, as listed in Table III, B-Ga binding is weakly attractive, and

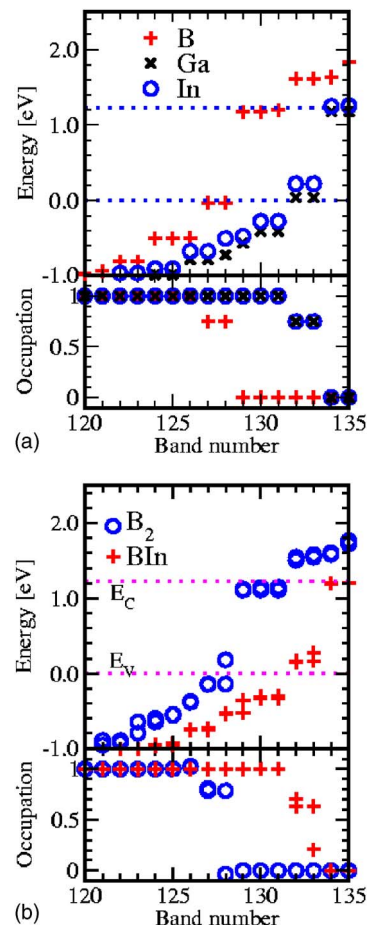


FIG. 6. (Color online) Density of states of single acceptors and acceptor-acceptor pairs. In  $B_2$ , acceptor states are located at the valence band maximum, but in BIn pair both holes occupy deep levels.

B-In has a substantial binding energy. We believe that the holes associated with B are well delocalized and thus ionized B atoms repel each other. However, in conjunction with the larger ionization energy, holes associated with In atoms (and to a lesser extent Ga) are more localized, and the localization is enhanced by the presence of an additional acceptor. Localized holes then stabilize the formation of B-In (and B-Ga) pairs. Figure 5 shows a comparison of hole distribution around B, In, and BIn. This mechanism is supported by the fact that removing the holes by considering negatively charged cells leads to elimination of B-In binding (Table IV), and previous theoretical work by Szmulowicz *et al.* found that BIn pair has large first ionization energy.<sup>25</sup>

Unlike donor-acceptor pairing, no charge compensation is involved, so acceptor-acceptor binding might be expected to lead to enhanced hole concentrations. Unfortunately, our calculations indicate that the BIn pair is a deep acceptor as shown in Fig. 6(b), with both acceptor levels located well within the gap. This prediction is supported by experimental results of Scalese *et al.*,<sup>10</sup> who found that In codoping deactivates B. However, as in the case of donor-acceptor pairing, In can be used to reduce B diffusion.<sup>6</sup>

#### IV. CONCLUSION

In conclusion, we investigated binding of various donor-acceptor pairs and acceptor-acceptor pairs and the resulting impact on the maximum charge carrier density. Counter doping B with As or Sb can reduce the junction depth due to retarded B diffusivity, but the calculated pairing effect is not large enough to overcome the charge compensation between opposite dopant types. Counter doping P with Ga or In, however, is predicted to enhance electron concentration via pairing of multiple P atoms with a single In or Ga atom, thereby providing an increase in the maximum concentration of the electrically active P which exceeds the compensation via the acceptors. BIn shows a surprisingly significant attractive binding, which we attribute to localized holes overcoming the expected ionized acceptor repulsion. However, B-In codoping leads to a reduced rather than an enhanced hole density since it produces deep acceptor levels. For both

donor-acceptor and acceptor-acceptor codoping, attractive binding is also expected to lead to a reduced diffusion and thus a more abrupt junction formation.

#### ACKNOWLEDGMENTS

This work was supported by the Semiconductor Research Corporation (SRC). We also thank Intel and AMD for donation of computer hardware used in this work.

- <sup>1</sup>E. Ganin, B. Davari, D. Hareme, G. Scilla, and G. A. Sai-Halasz, *Appl. Phys. Lett.* **54**, 2127 (1989).
- <sup>2</sup>S. Kwon, H. Kim, and J. Lee, *Jpn. J. Appl. Phys., Part 2* **29**, L2326 (1990).
- <sup>3</sup>S. Solmi, *J. Appl. Phys.* **83**, 1742 (1998).
- <sup>4</sup>C. Ahn, M. Diebel, and S. T. Dunham, *J. Vac. Sci. Technol. B* **24**, 700 (2006).
- <sup>5</sup>C. Ahn, J. Song and S. T. Dunham, *Mater. Res. Soc. Symp. Proc.* **913**, D05 (2006).
- <sup>6</sup>H. Li, T. A. Kirichenko, P. Kohli, S. K. Banerjee, R. Tichy, and P. Zeitzoff, *IEEE Electron Device Lett.* **23**, 646 (2002).
- <sup>7</sup>S. Solmi, S. Valmorri, and R. Canteri, *J. Appl. Phys.* **77**, 2400 (1995).
- <sup>8</sup>C. Revenant-Brizard, J. R. Regnard, S. Solmi, A. Armigliato, S. Valmorri, C. Cellini, and F. Romanato, *J. Appl. Phys.* **79**, 9037 (1996).
- <sup>9</sup>N. E. B. Cowern, *Appl. Phys. Lett.* **54**, 703 (1989).
- <sup>10</sup>S. Scalese, S. Grasso, M. Italia, V. Privitera, J. S. Christensen, and G. G. Svensson, *J. Appl. Phys.* **99**, 113516 (2006).
- <sup>11</sup>G. Kresse and J. Hafner, *Phys. Rev. B* **47**, 558 (1993); G. Kresse and J. Furthmüller, *ibid.* **54**, 11169 (1996).
- <sup>12</sup>D. Vanderbilt, *Phys. Rev. B* **41**, 7892 (1990); G. Kresse and J. Hafner, *J. Phys.: Condens. Matter* **6**, 8245 (1994).
- <sup>13</sup>A. Baldereschi, *Phys. Rev. B* **7**, 5212 (1973); D. J. Chadi and M. L. Cohen, *ibid.* **8**, 5747 (1973); H. J. Monkhorst and J. D. Pack, *ibid.* **13**, 5188 (1976).
- <sup>14</sup>M. Diebel, Ph.D. thesis, University of Washington, Seattle (2004).
- <sup>15</sup>R. W. Godby and M. Schlüter, *Phys. Rev. Lett.* **56**, 2415 (1986).
- <sup>16</sup>J. Lento, J.-L. Mozos, and R. M. Nieminen, *J. Phys.: Condens. Matter* **14**, 2637 (2002).
- <sup>17</sup>D. K. Sadana, A. Acovic, B. Davari, D. Grutzmacher, H. Hanafi, and F. Cardone, *Appl. Phys. Lett.* **61**, 3038 (1992).
- <sup>18</sup>K. Yokota, M. Ochi, T. Hirao, Y. Ando, and K. Matsuda, *J. Appl. Phys.* **69**, 2975 (1991).
- <sup>19</sup>M. Rudan and G. Perroni, *Semicond. Sci. Technol.* **19**, S82 (2004).
- <sup>20</sup>E. Atoro, Y. Ohama, and Y. Hayafuji, *Appl. Phys. Lett.* **83**, 3051 (2003).
- <sup>21</sup>S. Solmi, A. Parisini, R. Angelucci, A. Armigliato, D. Nobili, and L. Moro, *Phys. Rev. B* **53**, 7836 (1996).
- <sup>22</sup>M. Derdour, D. Nobili, and S. Solmi, *J. Electrochem. Soc.* **138**, 857 (1991).
- <sup>23</sup>L. Romano, A. M. Piro, M. G. Grimaldi, G. M. Lopez, and V. Fiorentini, *Phys. Rev. B* **71**, 165201 (2005).
- <sup>24</sup>S. Solmi, A. Parisini, M. Bersani, D. Giubertoni, V. Soncini, G. Garnevale, A. Benvenuti, and A. Marmiroli, *J. Appl. Phys.* **92**, 1361 (2002).
- <sup>25</sup>F. Szmulowicz, J. K. Wendeln, and S. C. Slaton, *J. Appl. Phys.* **55**, 2945 (1984).